

# **LED-based Standard Lamp for Realization of Photometric Units**

Johannes Oksanen

**School of Electrical Engineering**

Thesis submitted for examination for the degree of Master of  
Science in Technology.

Espoo 3.10.2016

**Thesis supervisor:**

Prof. Erkki Ikonen

**Thesis advisors:**

D.Sc. Tuomas Poikonen

M.Sc. Hans Baumgartner

Author: Johannes Oksanen

Title: LED-based Standard Lamp for Realization of Photometric Units

Date: 3.10.2016

Language: English

Number of pages: 6+41

Department of Signal Processing and Acoustics

Professorship: Measurement Science and Technology

Supervisor: Prof. Erkki Ikonen

Advisors: D.Sc. Tuomas Poikonen, M.Sc. Hans Baumgartner

Standard lamps of luminous intensity are widely used in the field of photometry as references or stable sources in calibration measurements and in realization of SI units. Due to the fact that the lighting industry is moving from incandescent and fluorescent lamps to LED-based lighting, a concern about the availability of the incandescent standard lamps has arisen. Laboratories have to develop new methods and equipment to measure new light sources, such as LEDs, which differ from the traditional incandescent lamps, especially in spectral and angular properties. According to a recently published study, spectral errors in photometric measurements of LEDs can be reduced down by a factor of 3 on the average, if incandescent calibration sources are replaced by LED-based sources in calibration of photometers. Recently, the development of white LEDs has produced a wide range of LEDs with increased optical output and different colour temperatures. Some of these LEDs may be suitable to be used as stable calibration sources.

In this work, a new LED-based luminous intensity standard lamp has been developed for use in photometric calibrations as a stable source of illuminance. The new source was characterised for temporal stability, spectral and angular properties, as well as for repeatability of luminous intensity. The LED-based standard lamp performed equally or better than a traditional Osram Wi41/G incandescent standard lamp. The expanded uncertainty of the luminous intensity measurement of the LED standard lamp is 0.62 % ( $k = 2$ ) at the distance between 0.5 m - 4 m.

Keywords: luminous intensity, photometry, illuminance, standard lamp

Tekijä: Johannes Oksanen		
Työn nimi: LED-valoon perustuva standardivalolähde valaistussuureiden realisointiin		
Päivämäärä: 3.10.2016	Kieli: Englanti	Sivumäärä: 6+41
Signaalinkäsittelyn ja akustiikan laitos		
Professuuri: Mittaustekniikka		
Työn valvoja: Prof. Erkki Ikonen		
Työn ohjaaja: TkT Tuomas Poikonen, DI Hans Baumgartner		
<p>Valovoimalamput ovat oleellinen osa valaistussuureiden realisointi- ja kalibrointi-laitteistoissa, joissa niitä käytetään standardilamppuina ja stabiileina valonlähteinä. Yleinen suuntaus on että valaistuksessa ollaan siirtymässä hehkulamputa ja loisteputkivalaisimista ledipohjaisiin toteutuksiin. Myös perinteisten standardi-hehkulamppujen valmistus loppuneen lähitulevaisuudessa. Standardilamppujen saatavuuden turvaamisen lisäksi laboratorioissa on kehitettävä menetelmiä ja laitteita, joilla voidaan tarkasti mitata uudentyyppisiä valonlähteitä, kuten ledejä, jotka poikkeavat perinteisistä valonlähteistä spektreiltään ja säteilykuvioiltaan. Äskettäin julkaistun tutkimuksen mukaan spektrisiä virheitä fotometrisissä mittauksissa voidaan vähentää keskimäärin kolmasosaan korvaamalla fotometrien kalibrointilähteinä käytetyt hehkulamput ledeillä.</p> <p>Viime aikoina markkinoille on tullut laaja valikoima valkoisia ledejä, jotka optisen tehon, spektrin ja eliniän perusteella sopivat hyvin standardilampun valonlähteeksi. Tässä työssä on kehitetty led-pohjainen valovoiman standardilamppu, jolle on suoritettu täydelliset karakterisointimittaukset. Lamppua voidaan käyttää fotometrian kalibroinneissa stabiilina valonlähteenä. Kehitetty lamppu karakterisoiittiin mittaamalla sen spektrinen irradianssi, säteilykuvio sekä lyhyen ja pitkän ajan stabiilisuus. Lisäksi tutkittiin toistuvuutta valovoiman mittauksissa. Mittausten perusteella ledistandardilampun stabiilisuus ja fotometriset ominaisuudet ovat vähintään yhtä hyvät tai paremmat kuin yleisesti käytössä olevilla Osram Wi41/G-hehkulampuilla. Kehitetyn standardilampun laajennettu epävarmuus valovoiman mittaukselle on 0.62 % (<math>k = 2</math>) etäisyydellä 0.5 m - 4 m.</p>		
Avainsanat: valovoima, photometria, valaistusvoimakkuus, standardilamppu		

# Contents

Symbols and abbreviations	v
<b>1 Introduction</b>	<b>1</b>
<b>2 Background</b>	<b>3</b>
2.1 Luminous intensity . . . . .	3
2.2 Realization of luminous intensity . . . . .	5
2.3 Requirements for a standard lamp . . . . .	8
<b>3 LED-based standard lamp for photometry</b>	<b>12</b>
3.1 Selection of the light emitting diodes . . . . .	14
3.2 Mechanical design . . . . .	17
3.3 Temperature control electronics . . . . .	18
3.4 Operating instructions for the LED source . . . . .	25
<b>4 Characterization results</b>	<b>27</b>
4.1 Ageing test for the LED modules . . . . .	27
4.2 Characterization of the LED standard lamp . . . . .	31
4.3 Measurement of luminous intensity . . . . .	34
4.4 Calibration of the integrating sphere . . . . .	36
<b>5 Conclusions</b>	<b>39</b>
<b>References</b>	<b>40</b>



# Symbols and abbreviations

## Symbols

$A_{\text{ext}}$	area of the limiting precision aperture
$c$	speed of light in vacuum $\approx 3 \times 10^8$ [m/s]
$E(\lambda)$	spectral irradiance
$d$	distance
$d_s$	distance from the source
$F$	colour correction factor
$h$	Planck constant
$i$	electrical current
$I_e$	radiant intensity [W/sr]
$I_v$	luminous intensity
$I_{v,\text{eff}}$	effective luminous intensity
$k_B$	Boltzmann constant
$K_m$	photopic normalization constant $\approx 683$ [lm/W]
$r_p$	effective radii of the photometer aperture
$r_s$	effective radii of the light source
$S_{\text{eff}}$	relatice distance
$s_{\text{rell}}$	spectral responsivity of a detector
$s(555)$	the absolute responsivity of the photometer at the peak wavelength, 555 nm
$T_c$	carrier temperature
$V(\lambda)$	relative spectral sensitivity of human eye
$\alpha$	self-absorption correction coefficient
$\lambda$	wavelength
$\Phi_{\text{cal}}$	the spectrum of the calibration source
$\Phi_{\text{source}}$	the spectrum of the measured lamp

## Abbreviations

ADC	Analog to Digital Converter
BaSO <sub>4</sub>	Barium sulfate
CCT	Correlated Color Temperature
CIE	Commission Internationale de l'Éclairage,

	International Commission on Illumination
LED	Light Emitting Diode
MRI	Metrology Research Institute
PQED	Predictable Quantum Efficient Detector
SSL	Solid State Lighting
SI	Système international d'unités

# 1 Introduction

Luminous intensity is the primary quantity of photometry. The unit of luminous intensity is candela [cd] which is the part of the International System of Units (SI).

For decades, incandescent lamps have been used not only in lighting but also as standard sources of luminous intensity in calibration of photometric equipment. Due to the development of solid state lighting and energy saving related legislation, incandescent lighting is phasing out. It could be argued that manufacturing of incandescent standard lamps may end in the near future as well. That is to say, incandescent standard lamps need to be replaced with LED based standard lamps in order to continue photometric calibration work.

In addition to the possible availability problem, there is another reason to use LED lamps instead of incandescent lamps as the standard in calibrations. According to a recently published article [1], use of an LED-based standard lamp would provide reduced spectral errors, if the standard lamp and the measured light have similar spectra. White LED-lamps can be roughly divided into "warm white" and "cold white" lamps based on their correlated colour temperatures (CCT). That is, minimum of two different colour temperatures are required for LED based calibration sources in order to calibrate photometers for measurement of typical LED lighting: "illuminant  $L_W$ " with a colour temperature of approximately 3000 K and "illuminant  $L_C$ " with a colour temperature of approximately 6000 K describing typical warm and cold white LEDs, respectively.

LED lamps are already proven to be suitable for calibration and laboratory use. For example, an LED-based luminous intensity standard and luminance standard are reported in [1, 2]. Different types of LED-based standards and calibration lamps are already developed and published in [3, 4]. Sametoglu et al. [3] used white LEDs as a source when investigating photometric errors of commercial photometers. Fryc et al. [4] built a spectrally tunable light source utilizing LEDs with different colours which can approximate various CIE daylight illuminants.

In this work, an LED-based standard lamp was developed and characterised for spectral and angular properties, as well as for repeatability of luminous intensity. It consists of two LED modules with different colour temperatures, a thermoelectric module based on cooler-heater and a temperature stabilizer electronics. The LED-based standard lamp was designed to directly replace traditional incandescent lamps in photometric calibrations so that no optical or mechanical changes to the existing measurement setups are required. That is to say, the new standard lamp can be used as a standard lamp for luminous intensity or as a stable source in calibrations of photometers or other measurement facilities, such as integrating spheres. In the

near future, the LED-based standard lamp will be used with a predictable quantum efficient detector (PQED), the photometer of the future.

The developed standard lamp is compared against a traditional incandescent standard lamp and results are presented. In addition, ten Chip-on-Board-type (COB) LEDs which are of the same type as the one used in the developed standard lamp were aged over a 4 months period in order to examine long term stability and ageing of the source.

## 2 Background

In this section, basics of the realization of luminous intensity and luminous flux units are discussed. Before designing a LED-based standard lamp, it is necessary to understand what luminous flux is and how it is defined, what kind of lamps are used as standards and how they are used in practical calibrations. It is also important to study the properties of LEDs on the market to find out which, if any, of them are suitable for the purpose.

### 2.1 Luminous intensity

Luminous intensity is the primary quantity of photometry in the field of optical metrology. The unit of luminous intensity is determined by International Committee for Weights and Measures (CIPM) as an intensity, emitted by a monochromatic, light source with a frequency of 540 THz and with a radiant intensity of 1/683 watts per steradian in a given direction [5]. The luminous intensity for nonmonochromatic light can be expressed as

$$I_v(\lambda) = K_m \int_0^\infty V(\lambda) I_e(\lambda) d(\lambda), \quad (1)$$

where  $K_m$  is the maximum spectral luminous efficacy of radiation for photopic vision ( $683 \frac{\text{lm}}{\text{W}}$ ),  $I_v$  is the luminous intensity in candelas,  $I_e(\lambda)$  is the spectral radiant intensity in watts per steradian, and  $V(\lambda)$  is the relative spectral responsivity of a human eye.

In laboratories, luminous intensity can be measured using a photometer based on a silicon photodetector. The photometer converts the incident spectral radiant flux to electrical current  $i$ . For example, to realize candela at Metrology Research Institute (MRI), a photometer comprising of a silicon photodetector,  $V(\lambda)$ -filter and a precision aperture are placed next to a light source and the luminous intensity is calculated as

$$I_v = \frac{K_m S_{\text{eff}}^2}{A s(555)} F i, \quad (2)$$

where  $A$  is the area of the limiting aperture,  $S_{\text{eff}}$  is the effective distance between the receiving plane of the photometer and the emitting surface of the source, and  $s(555)$  is the absolute responsivity of the photometer at the peak wavelength, 555 nm, of the  $V(\lambda)$  function.

The colour correction factor  $F$  describes the effect of the difference between the theoretical  $V(\lambda)$  function and the relative spectral responsivity  $s_{\text{rel}}(\lambda)$  of the photometer. The colour correction factor is the ratio of two integrals

$$F = \frac{\int \Phi_{\text{cal}}(\lambda) V(\lambda) d\lambda}{\int \Phi_{\text{cal}}(\lambda) s_{\text{rel}}(\lambda) d\lambda}, \quad (3)$$

where  $\Phi_{\text{cal}}$  is the spectrum of the calibration source and  $s_{\text{rel}}$  is the spectral responsivity of the detector.

For an ideal photometer with a perfect  $V(\lambda)$  filter, the colour correction factor would be unity for all sources. However, any photometer is ideal and the colour correction factor has to be determined. Especially when using a calibrated photometer to realize units such as luminous flux or to calibrate other light sources, the colour correction factor starts to have a significant influence on the uncertainty of measurement results.

Equation (3) applies to measurements made with fully characterized detectors. At Metrology Research Institute (MRI), a custom made detector has been built and the response of its photodiode and the transmittance of its  $V(\lambda)$ -filter are measured separately. Thus the custom made detector can be used as a standard for measuring the illuminance of light sources, and it is used as a reference photometer, against which all working standard photometers are calibrated.

Illuminance  $E_v$  is the total luminous flux incident on a surface per unit area. The unit for illuminance is lux [lx] or lumens per square metre  $\frac{\text{lm}}{\text{m}^2}$  and the relation between the measured photocurrent  $i$  and the illuminance  $E_v$  can be written as

$$E_v = \frac{K_m}{As(555)} Fi. \quad (4)$$

A typical calibrated reference photometer consists of a precision aperture, a photometric  $V(\lambda)$ -filter and a silicon photodiode. At present, all photometers are calibrated against an incandescent lamp with the Standard Illuminant A spectrum with a CCT of 2856 K. However, typically the light source to be measured using the calibrated photometer has a spectrum totally different from the Standard Illuminant A spectrum. In addition to the spectral mismatch between the ideal  $V(\lambda)$  function and the responsivity of the photometer, an additional spectral mismatch due the spectral error which arises when the calibrated photometer is used to measure light sources whose spectral power distributions deviate from that of the calibration source. The spectral error can be taken into account through a spectral mismatch correction factor

$$F_2 = \frac{\int \Phi_{\text{source}}(\lambda) V(\lambda) d\lambda}{\int \Phi_{\text{source}}(\lambda) s_{\text{rel}}(\lambda) d\lambda} \cdot \frac{\int \Phi_{\text{cal}}(\lambda) s_{\text{rel}}(\lambda) d\lambda}{\int \Phi_{\text{cal}}(\lambda) V(\lambda) d\lambda}, \quad (5)$$

where  $\Phi_{\text{source}}$  is the spectrum of the measured lamp.

As can be seen from equation (5), colour correction factor  $F_2$  is close to unity when

terms  $\Phi_{\text{source}}$  and  $\Phi_{\text{cal}}$  are close to each other. In this work we have developed two LED-based illuminant standard lamps providing two different colour temperatures. These warm white and cool white LED based illuminants are referred as Illuminant  $L_W$  and Illuminant  $L_C$  and the correlated colour temperatures for Illuminants  $L_W$  and  $L_C$  are approximately 3000 K and 6000 K, respectively. According to Pulli et al. [1], the use of an LED lamp with illuminant  $L_W$  or  $L_C$  spectrum as a calibration source instead of illuminant A, reduces spectral mismatch errors down to 1/3 on average, when incandescent standard lamps are replaced by LED-based standard lamps in calibrations of photometers.

In addition to being a luminous intensity standard lamp, the developed lamp can be utilized as a stable external source for luminous flux realization with an integrating sphere. For luminous flux measurements carried out in an integrating sphere, the colour correction factor is calculated using the equation

$$F_3 = \frac{\int \Phi_{\text{source}}(\lambda) \cdot V(\lambda) d\lambda}{\int \Phi_{\text{source}}(\lambda) / \alpha \cdot s_{\text{rel}}(\lambda) \cdot T(\lambda) d\lambda} \cdot \frac{\int \Phi_{\text{source}}(\lambda) / \alpha(\lambda) d\lambda}{\int \Phi_{\text{source}}(\lambda) d\lambda} \cdot \frac{\int S_r(\lambda) \cdot s_{\text{rel}}(\lambda) \cdot T(\lambda) d\lambda}{\int S_r(\lambda) \cdot V(\lambda) d\lambda} \quad (6)$$

where  $T(\lambda)$  is the spectral throughput of the integrating sphere,  $\alpha$  is a self-absorption correction coefficient and  $S_r(\lambda)$  is the spectrum of the external standard source [6]. As can be determined from equation (6), when measuring LED light sources  $\Phi_{\text{source}}$ , the colour correction factor (6) can be made close to 1 by using an LED based external standard source  $s_r$ .

## 2.2 Realization of luminous intensity

Realization of luminous intensity and calibration of photometric equipment can be carried out with two different methods: source based or detector based. In the source based method, the light source is used as a standard of the calibration with a known value of luminous intensity. In the detector based method, the detector works as a reference with known illuminance responsivity.

At MRI, the realization of photometric units is based on the detector based method. The setup comprises a reference photometer, a light source and a distance-measurement system. In addition, a baffle and an alignment system are typically used. Figure 1 shows the measurement setup used for luminous intensity calibrations at MRI.

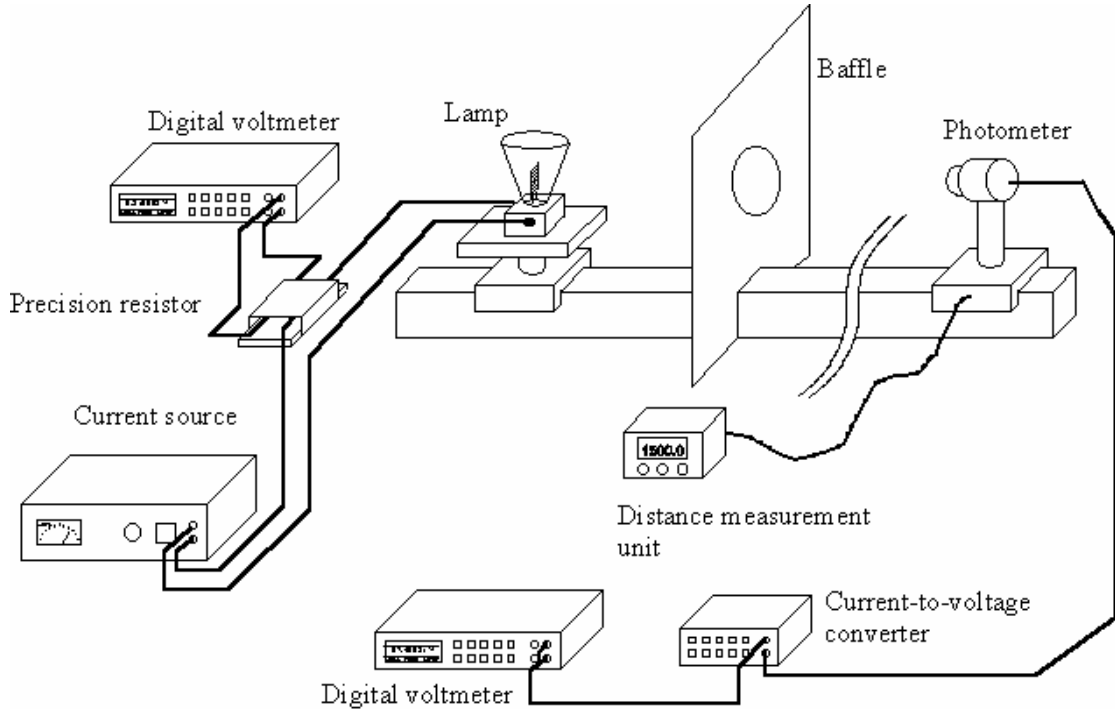


Figure 1: The detector based luminous intensity realization setup at MRI [7].

In figure 1, the lamp is placed on the optical rail equipped with a magnetic distance measurement unit. Voltage over and current through the lamp are measured with a digital volt meter utilizing a precision resistor. The photometer is a temperature stabilized trap detector with a  $V(\lambda)$ -filter. The weak current signal from the photometer is converted into voltage using a current-to-voltage converter and the voltage is read using the digital voltmeter. The baffle is used to block the scattered light.

As discussed in Chapter 2.1, custom made detectors are used at MRI. The reference photometer consists of a trap detector, a  $V(\lambda)$ -filter and a precision aperture. Together with the distance measurement system, these components create the realization setup for the luminous intensity. The trap detector is calibrated against a cryogenic radiometer, the  $V(\lambda)$ -filter is calibrated using the reference spectrometer of MRI and the area of the aperture and the distance measurement unit are calibrated by MIKES.

A typical luminous intensity standard lamp is a cone or "mushroom" shaped incandescent lamp. Metrology Research Institute uses Osram Wi 41/G lamps which have a maximum power rating of 180 W. The cone is covered with black paint except the front side in order to block diffused light. The filament is bent and forms a



flat square-shaped light source area. The output radiation of an incandescent lamp, such as Osram Wi 41/G, follows the inverse-square law. Osram Wi41/G and two other types of luminous intensity standard lamps, Polaron lamps and SIS 40-199, are represented in figure 2.



Figure 2: Different types of incandescent standard lamps (from left to right): Osram Wi41/G, Polaron and SIS 40-100 [8].

The luminous intensity lamp, working as a light source, is operated using a high quality DC power supply. The illuminance responsivity of the reference photometer has to be known as it works as a calibrated standard for the measurement. In the detector based method, other photometers can be calibrated against the lamp after it is measured with the reference photometer. For example, MRI and National Institute of Standards and Technology use this kind of detector based method to realise luminous intensity [9, 7].

In source based setups, the luminous intensity standard lamp works as a calibrated standard and it is measured with a stable detector. As contrast to the detector based method, other lamps, such as working standard lamps, can be calibrated with this kind of method. Alternatively, other working standard photometers can be directly compared to the reading of the reference photometer when using the lamp only as a stable source with known CCT, typically CIE Standard illuminant A.

In this work, a direct replacement of the incandescent lamp is developed. Therefore, optical and mechanical design need to be compatible with incandescent standard lamps and all typical detectors.

In addition to illuminance measurements on the optical rail, luminous intensity standard lamps are used with integrating spheres as stable external sources [10, 11] and in goniometers, such as the robot goniometer of Physikalisch-Technische Bundesanstalt (PTB) [12]. The LED-based standard lamp can be used in these applications. In this work, a new LED-based photometric standard lamp is developed mainly for illuminance measurements on the optical rail in calibration of the photometer illuminance responsivity. Characterization of the luminous flux responsivity of the 1.65 m- integrating sphere of MRI using the developed standard lamp as a stable external source is studied as well.

### 2.3 Requirements for a standard lamp

The emission spectra of an incandescent lamp and an LED are based on different phenomena. Incandescent lamps consist of a resisting wire which glows due to the high temperature inside a vacuum bulb producing light and also heat. The spectrum of the radiated light can be determined from the Planck law [13, p. 5]

$$I_v(T, \lambda) = \frac{2hc^2}{\lambda^5} \frac{1}{e^{\frac{hc}{\lambda k_B T}} - 1} \quad (7)$$

where  $h$  is the Plank constant,  $c$  is the speed of light,  $\lambda$  is the wavelength,  $k_B$  is Boltzmann constant and  $T$  is the temperature.

Planck law applies only for an ideal black body whereas an incandescent lamp is a grey body. For incandescent lamps, the Wien radiation law gives a sufficient representation of the black body radiation [13, p. 5]. It is written as

$$I_v(T, \lambda) \approx \frac{2hc^2}{\lambda^5} e^{-\frac{hc}{\lambda k_B T}} \quad (8)$$

In contrast to incandescent lamps, LEDs are semiconductors and emit photons when a radiative recombination of an electron-hole pair occurs in semiconductor material [14, p. 27]. The energy of the emitted photon is

$$E_g = h\nu, \quad (9)$$

where  $\nu$  is the frequency of the emitted photon. The wavelength of the photons can be determined from this equation [14, p. 27]. The spectrum of an LED is broadened around the peak wavelength depending on the semiconductor materials used. A

single LED can not produce white light, thus a phosphor layer or several layers are placed on top of the semiconductor material. The phosphor layer works as a wavelength-converter absorbing high-energy photons and emitting photons at lower energies. Therefore, the spectrum of a white LED consists of a blue peak which is produced by the LED chip itself and broadened at higher wavelengths. As a result, a blue LED with the phosphor layer produces white light.

High power LEDs in various different colours have been in the market for a while, hence a vast selection of LEDs with different specifications is available. LEDs are different kind of light sources than incandescent lamps when comparing spectra or spatial distributions. This may cause challenges when designing a fully compatible successor for a luminous intensity standard lamp, such as Osram Wi41/G. Despite the light spectrum, the mechanical and optical properties of an LED-based standard lamp need to be similar to the incandescent standard lamps. This is to ensure compatibility with existing measurement facilities.

Especially, the typical mismatch between the optical and mechanical axis of an LED is a drawback which is mainly caused by the lens on the top of the LED chip [15]. Therefore, chip on board (COB) LEDs were under our interest in this work, as they omit the use of a lens on top of the LED. A COB-style LED, such as Osram Soleriq, has no lens but only a flat surface as a light source. The shape of the light source is similar to a light source area of Osram Wi41/G and a lenseless design indicates an un-collimated beam. This gives a possibility that the COB-style LED is a Lambertian source hence fitting well the inverse-square law.

For LEDs having a lens (typically a drop of epoxy), an equation for the illuminance produced by the LED is developed which takes into account the difference between the physical and optical source of the LED [16]. In practise, it is a modified inverse-square law, which has terms for distance correction. The equation assumes an LED as a virtual source which is homogeneous and aligned in the centre of the optical axis of the measurement system. The equation for the LED illuminance is

$$E_v(d) = \frac{I_{v,\text{eff}}}{(d + \Delta d_s)^2 + r_s^2 + r_p^2} g(d), \quad (10)$$

where  $d + \Delta d_s$  is the physical distance between the virtual source of the LED and the aperture plane of the photometer,  $I_{v,\text{eff}}$  is the effective luminous intensity of the extended LED virtual source on the measurement axis,  $r_p$  and  $r_s$  are the effective radii of the virtual source and photometer aperture [16]. Factor  $g(d)$  is neglected due to the fact that it is near 1. Equation (10) points out the problem with LEDs and the inverse-square law: An LED, especially with a lens, may not be a point source, and may be difficult to use as a standard for luminous intensity, or as a stable source

for illuminance in photometric calibrations, due to possible alignment problems.

Good stability is a necessary attribute for a standard lamp. Actually, two different types of stabilities can be discussed: Long term stability which means maintenance of luminous intensity and spectral properties over several years. Short term stability which means that measured illuminance and spectrum of the lamp are stable over a time of each calibration measurement, for example, between comparing the readings of two detectors.

Ageing and stability of LEDs are widely studied recently and several publications are published about the ageing of high power white LED chips or lamps [17, 18, 19]. These studies show that LED chips or lamps have a lifetime expectation more than 10 000 hours which is more than ten times higher than the lifetime expectation of existing incandescent standard lamps.

Furthermore, ageing studies show that high temperature reduces the lifetime [14, 17]. Therefore, low thermal stress is desirable and will extend the lifetime of the LED chip, which is important for a standard lamp.

Temperature stabilization is necessary, because electrical and optical properties of LEDs are strongly temperature depended [14]. That is to say, the internal quantum efficiency is commensurate to temperature.

A general equation for the emission intensity temperature dependence is

$$I \propto \exp\left(\frac{-hv}{kT_c}\right), \quad (11)$$

where  $T_c$  is the carrier temperature [14] being the upper limit for the junction temperature [14]. Close to the room temperature, the emission thermal dependency can be written as

$$I = I_{25^\circ C} \left( e^{\frac{-(T-25^\circ C)}{T_{cha}}} \right), \quad (12)$$

where  $I_{25^\circ C}$  is the emission intensity at 25 °C and  $T_{cha}$  is the characteristics temperature [20].

From equations 11 and 12, and from the fact that temperature reduces the lifetime of an LED, one can determine that the junction temperature of the LED used in the standard lamp should not be too high.

In this work, the temperature of the LED is not determined by calculations, because it is enough to stabilize it to a sufficient value. A sufficient value in this case is a temperature between 30-40 °C because ageing of the LED is then lower than in higher temperatures [17, 21]. The final selection of the temperature and the forward voltage is discussed later in this paper. Not only lifetime of solid state material

is a problem but also yellowing of epoxy [19, 22]. This phenomenon is caused by ultraviolet part of the intense blue light [22]. However, yellowing is not an issue with COB-type LEDs, because there is no a epoxy lens.

### 3 LED-based standard lamp for photometry

A new LED-based luminous intensity standard lamp was developed. Backwards compatible mechanics were developed to operate the new lamp with existing measurement setups. Due to the temperature sensitivity of the intensity and spectral properties of LEDs, temperature stabilizing electronics were also developed. In addition to the temperature stabilization electronics, a separate high quality constant current power supply is required to operate the LED unit. This chapter presents the details of the mechanical design of the developed standard lamp, as well as the documentation for the temperature stabilizing electronics. Furthermore, practical operation instructions of the standard lamp are documented in detail.

The LED-based standard lamp consists of a control unit, a cooling unit, and a replaceable LED-unit. The components of the developed LED standard lamp are presented in figure 3. The control unit consists of a 12-volt power supply, analog feedback measurement electronics, and a digital PID controller. The control unit stabilizes the voltage over the constant current driven LED-unit by controlling the temperature of the heat sink. Stabilizing the voltage over the LEDs, stabilizes also the electrical power and thus the luminous intensity of the LED. The operational principle of the control unit is explained in Chapter 3.3. The cooling unit is based on a thermoelectric module (TEM) which is mounted on a heat sink with backwards compatible mounting and alignment mechanics. Due to the requirements set by different types of LED modules, the LED-unit can be removed and replaced. High quality shielded cables with Lemo-connectors are used to interconnect the LED mounting base and the temperature control electronics unit. Two separate cables are used to prevent the crosstalk between the high power TEM current wires and the signal wires for the voltage and temperature measurements.

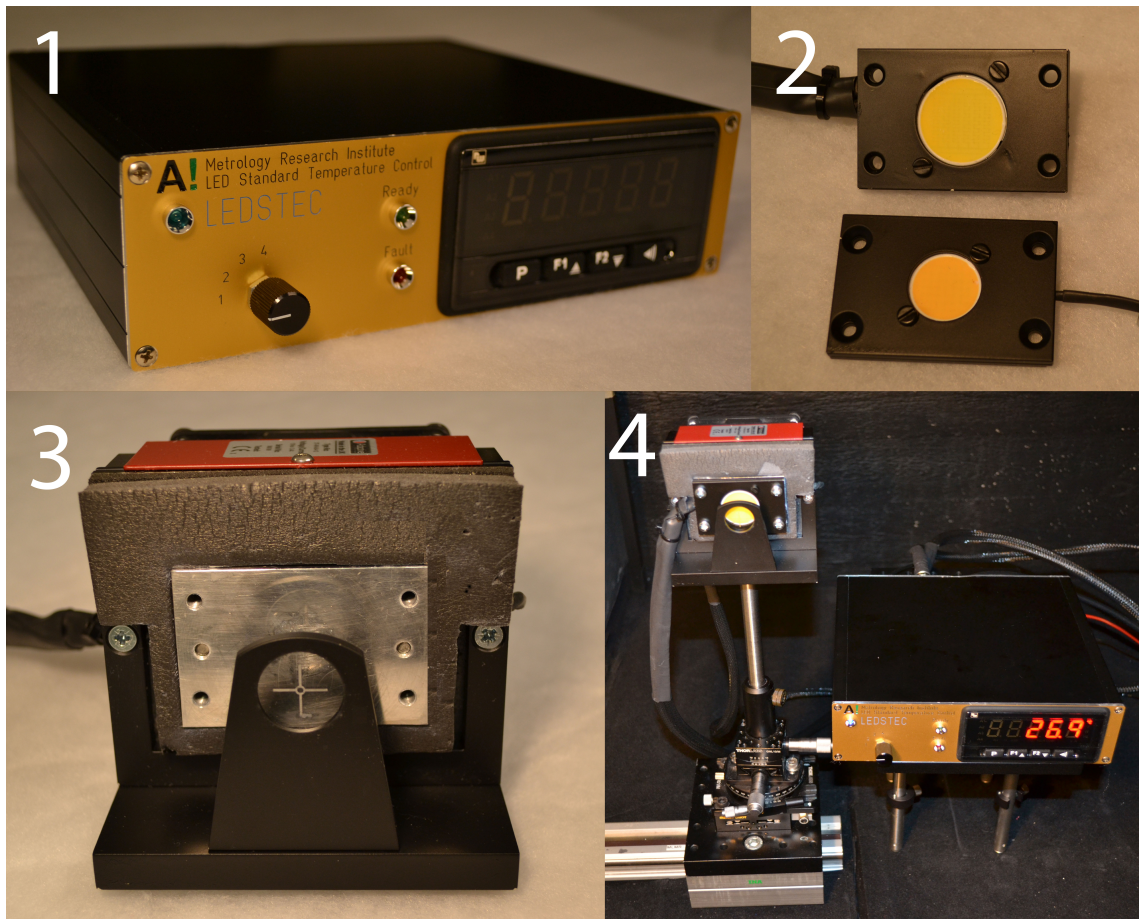


Figure 3: 1. a temperature control unit 2. two LED units 3. a cooler unit with an optical target 4. The standard lamp assembled on the optical rail.

### 3.1 Selection of the light emitting diodes

The LED luminous intensity standard was developed in order to achieve similar optical and mechanical properties as with incandescent standard lamps, excluding the spectral properties, which vary from the illuminant A spectrum of an incandescent standard.

After an overview on the LED market, two candidate LEDs were selected: Osram Soleriq and Ledengin LZ4-40R200. Both modules are based on high power white LEDs, capable of producing luminous intensity comparable to incandescent standard lamps. Spectra of the candidate LEDs were also suitable and colour temperatures were close to the CCTs of 3000 K and 6000 K, producing warm and cold white spectra. At the beginning of the project, preliminary test measurements were performed in order to find out which of the selected candidates are suitable for using as luminous intensity standard source, if any. Those test measurements were: colour temperature, inverse square-law, intensity and angular responsivity. Due to the fact that Soleriq does not have a lens on the solid state chip, it is assumed to be more lambertian source than Ledengine.

In the beginning of the project, preliminary tests were performed in order to establish which one of the selected candidates are suitable for the purpose. The candidate LEDs are presented in figure 4. Those test measurements were: colour temperature, fitting of the inverse square-law, in analysis of luminous intensity and the angular intensity distribution. Due to the fact that the Soleriq does not have a lense on the top of the solid state chip, it was assumed to be more Lambertian source than the Ledengine. The surface areas of the two Osrams are closer to the effective area of Osram Wi41/G. The picture also shows the problem with Ledengine: due to the lens, the LED chips look like bent, and might cause problems in alignment or fitting of the inverse square law.



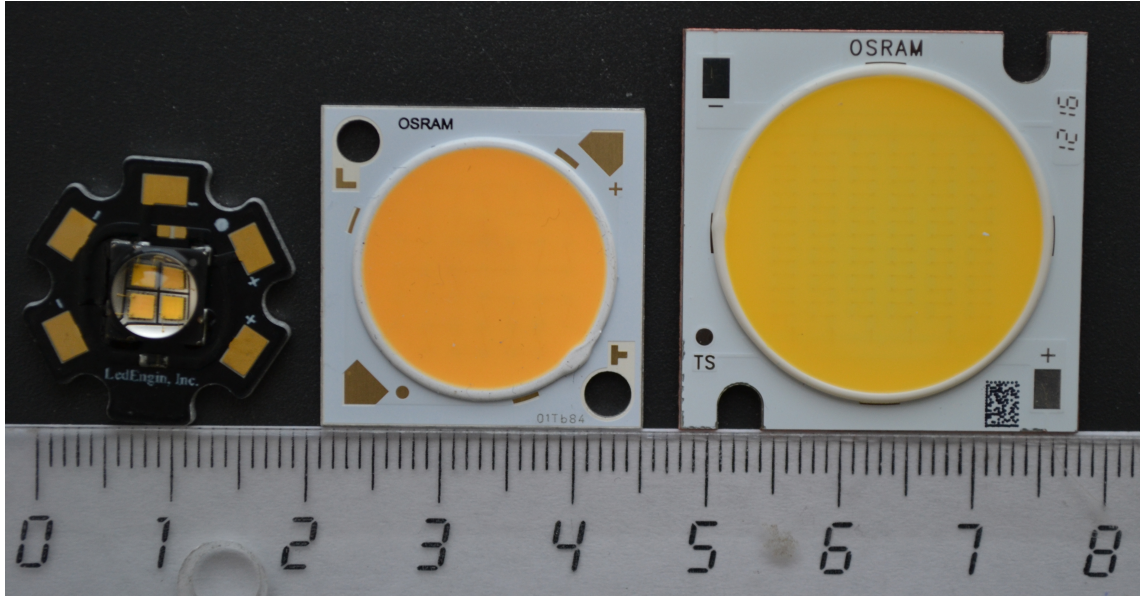


Figure 4: Photograph of the LED candidates that were chosen for preliminary testing. From left to right: Ledengin LZ4-40R200, Osram Soleriq warm white and Osram Soleriq cold white.

The angular intensity distributions were measured on the 5 m optical rail of MRI which is presented in Chapter 2.2. Figure 5 presents the angular intensity distributions for the three different types of LED modules measured. As can be seen from figure 5, due to the optical lens of the Ledengin module, its angular distribution is less Lambertian compared to the angular distributions of the Osram modules. Mismatch between the optical and mechanical axis is typical problem with LEDs that have lenses [15, 16]. In addition to the asymmetric distribution of the Ledengin LZ4-40R200, its colour temperature changes asymmetrically. For Ledengin, colour temperature is 3001 K at  $0^\circ$ , 2898 K at  $10^\circ$  and 2985 K at  $-10^\circ$ . For Osram Soleriq Cold White 5566 K, 5562 K and 5564 K and warm white 3154K, 3158K and 3154K, respectively. Spectra of the three candidates measured from three different angles for each are presented in figure 6.

On this basis, the Soleriq is much more suitable for use in a standard lamp, because it reduces the uncertainties due to alignment of the source drastically compared to the Ledengin. The measured CCT changes of the Soleriq as a function of angle of observation are similar to typical luminous intensity standard lamps, such as the Osram Wi41/G. Hence, Osram Soleriq is selected.

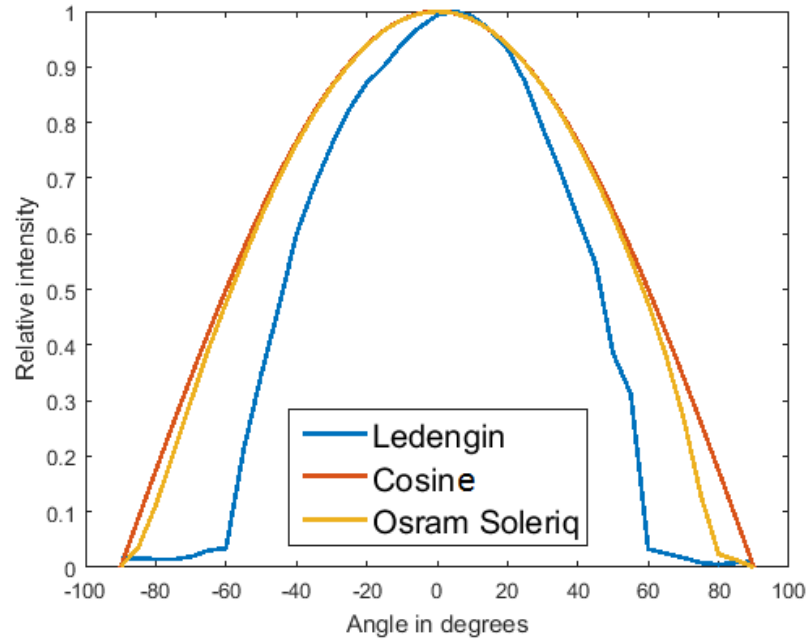


Figure 5: Relative angular intensity distribution of the LED candidates compared to the ideal cosinusoidal distribution of a Lambertian light source.

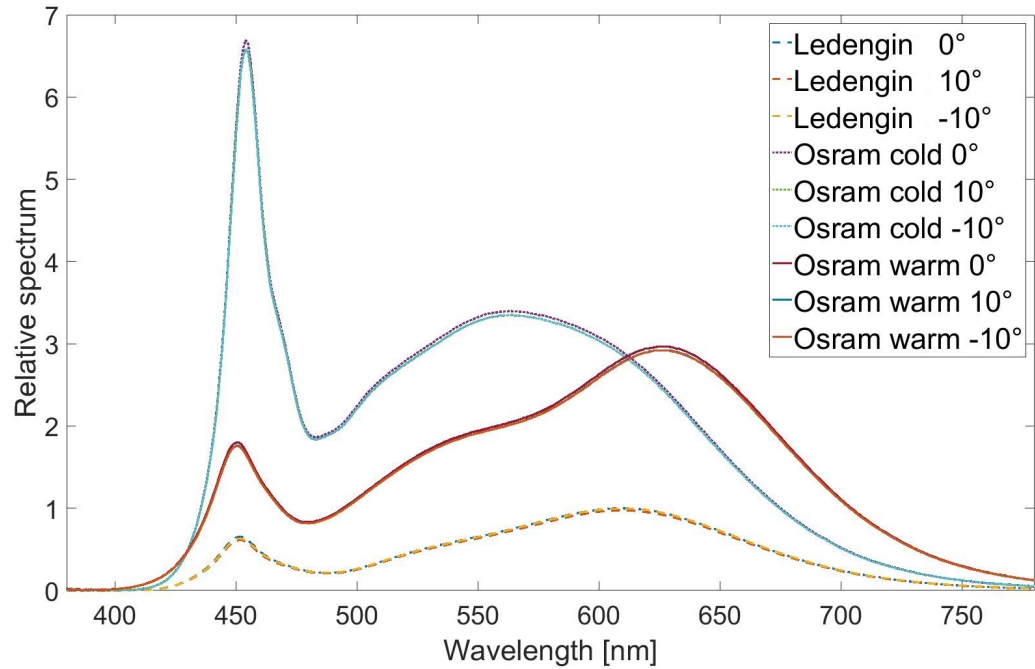


Figure 6: Relative spectral intensities of the LED candidates measured in 0° and 10° angles with respect to the optical axis of the LED.

### 3.2 Mechanical design

The mechanical parts of the new standard lamp were designed to make alignment and distance measurement straightforward and to be compatible with the existing measurement setups at MRI. The optical alignment jig and the front of the base plate were precision machined hence working as a reference surface. The optical target was precision machined aluminium and the target was a laser engraved acrylic.

Figure 7 shows the mechanics of the LED-based standard lamp. The optical target (1) has a reflective acrylic aim with a cross pattern. Using a reflectance acrylic as an aim makes it possible to use the reflective beam as assistance when aligning the lamp using an alignment laser. The body of the cooling unit (2) has M6 screws at the bottom, thus it can be mounted using typical mechanical parts used in laboratories. The aluminium parts were anodized and dyed black in order to prevent reflections which may hinder measurements. The front surface of the body works as a mechanical reference surface for the distance measurement.

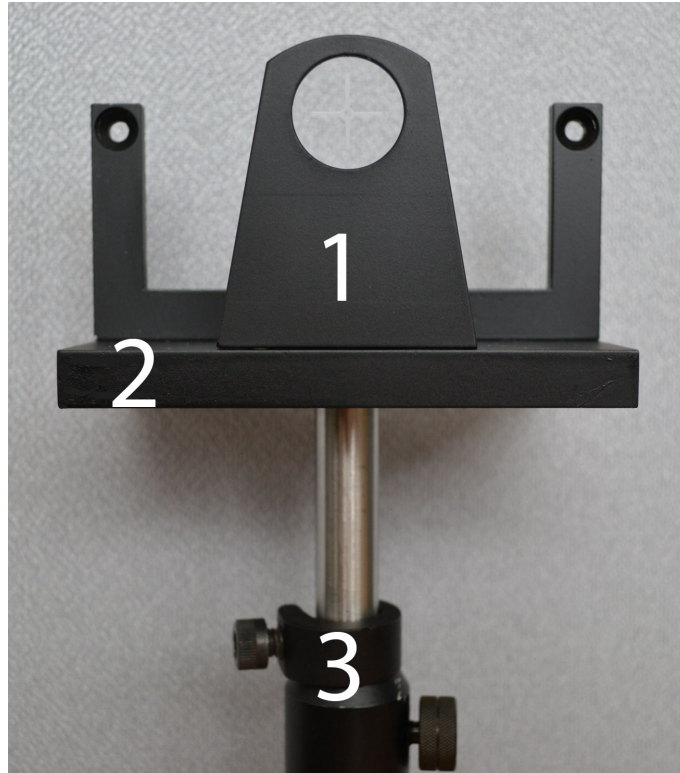


Figure 7: The mechanics of the LED-based standard lamp.

### 3.3 Temperature control electronics

Due to the temperature sensitivity of the LED spectra, the junction temperature of the LEDs need to be limited and stabilised in order to achieve stable operational conditions and long lifetime. Special temperature stabilizer electronics were designed to drive the Peltier element of the LED mounting holder. In the design, attention was paid to achieve durable and noise-free conditions on the circuit board. The device was built using high quality parts, such as a precision low drift instrumentation amplifier and thin film resistors with small temperature drift.

As the forward voltage of an LED follows the temperature over the pn-junction, the LED itself can be used as a relative temperature sensor [14]. Taking into account that the LEDs are driven using DC current, the voltage over the LED is the measurand to be stabilized and no additional temperature sensor was necessary. The thermal control unit measures the voltage over the LED module and controls the temperature of the LED unit. Stabilizing the forward voltage of the LED module, constant electric power and luminous output are achieved. In addition to the temperature feedback, the forward voltage over the LED module, signals stability of the LED module to the user with indicator LEDs. The working principle of the thermal control unit is shown in figure 8.

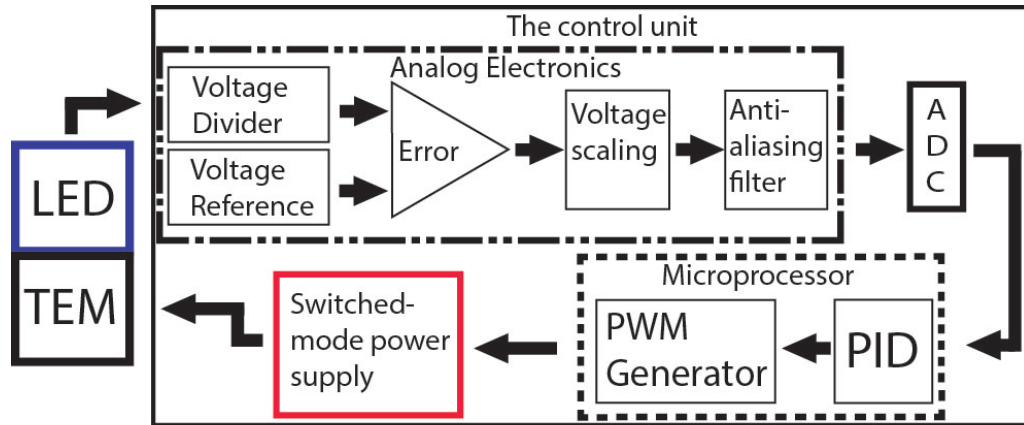


Figure 8: Working principle of the temperature control unit of the LED standard lamp.

The circuit board inside the temperature control unit is divided into two separate sections in order to avoid electronic disturbances between the power electronics driving the Peltier cooler and the feedback signals. The digital microprocessor taking care of the PID control and signal processing was installed as a separate circuit board on top of the analog circuit board using pin headers. The PWM signal from the PID



differential mode, it converts the difference of two input signals to a 16-bit signed integer. The other input of the ADC was the signal to be converted and the other input a constant reference voltage. When the input signal to be measured was smaller than the reference signal, the output of the ADC was a negative integer and vice versa.

The bipolar output voltage from "IC1" was converted to a positive voltage signal between 0 - 2.5 volts by adding a 1.25 volts offset voltage to the measurement signal. Figure 10 shows the circuit used to produce a high precision 1.25 volts offset voltage and the circuitry used to connect the voltage to the measurement signal.

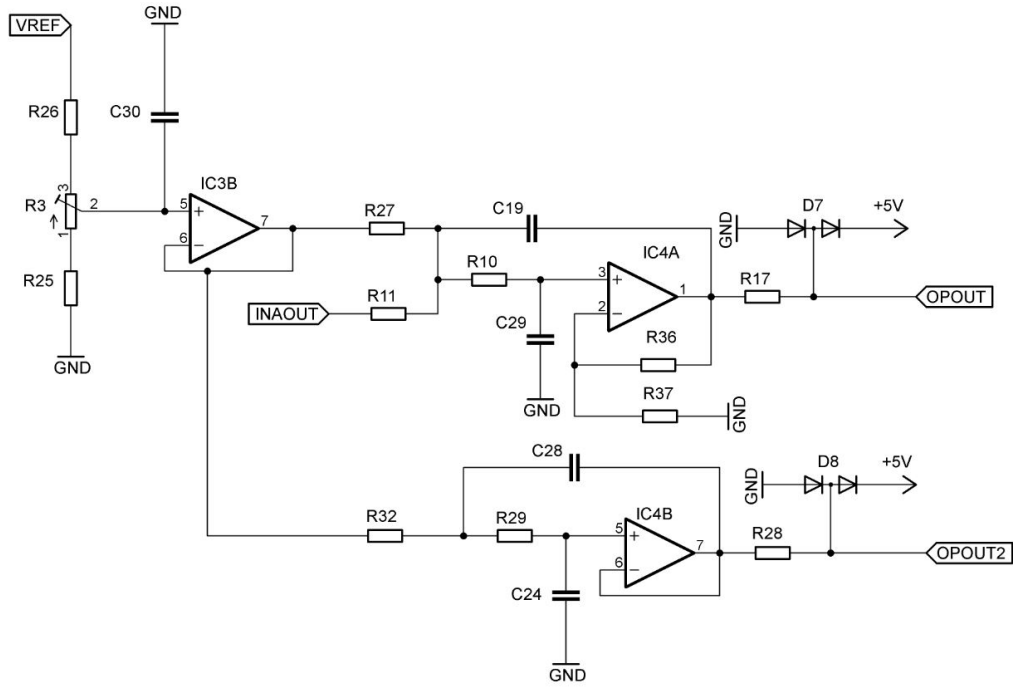


Figure 10: Schematics of the circuit to scale the error signal "INAOUT" from "IC1" to 0-5 V signal, suitable for the analog-to-digital converter.

As can be seen in figure 10, the 1.25 V offset voltage is adjusted using the trimmer potentiometer "R3" as a voltage divider. In addition to offset voltage for the measurement signal, the high precision 1.25 V voltage signal was also used as the other differential input signal for the analog-to-digital converter. This ensures that a zero volts error signal from "IC1", representing no error between the set point and the LED voltage, will be interpreted as 0 at the analog-to-digital converter, independent on the accuracy of the 1.25 V reference offset voltage. The operational amplifier "IC3" is used as a unity gain buffer for the 1.25 V offset voltage. The voltage "VREF" is the 10 V reference voltage produced by "IC8".

The operational amplifier circuits in 10 provides unity gain second order Sallen-Key low pass filters for the error and offset signals. Using the resistors and capacitors (C19, C29, C28, C24, R10, R11, R36, R37, R29, R32), the cutoff frequencies of the filters were set to 15 Hz. The output signals from the analog signal path "OPOUT" and "OPOUT2" are used as inputs for the analog-to-digital converter and their differences converted to 16-bit signed integer values. Figure 11 shows the schematics for the analog-to-digital converter.

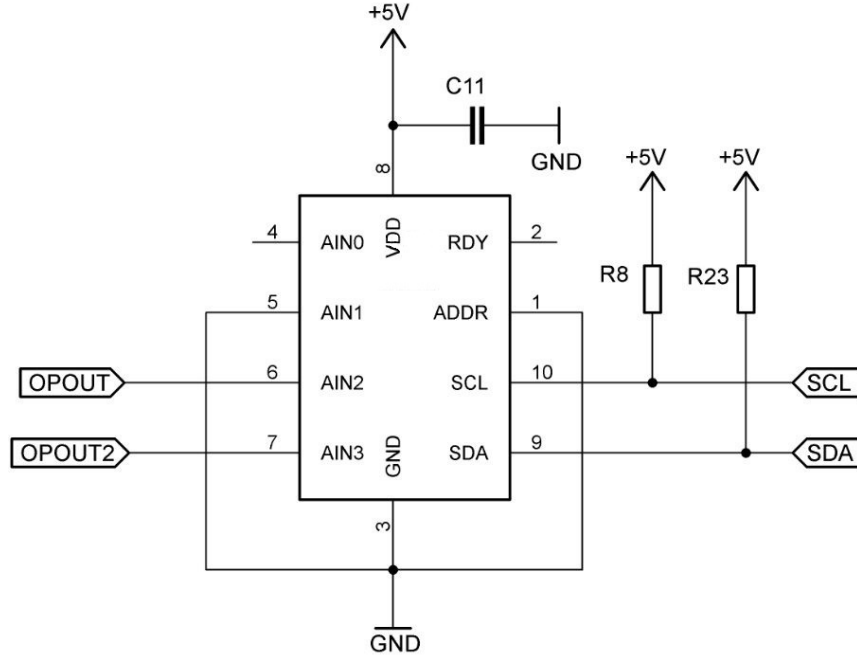


Figure 11: Texas Instruments ADS1115 analog-to-digital converter was used to convert the scaled error signal to 16-bit digital word for the processor

The voltage difference between "OPOUT" and "OPOUT2" is converted to 16-bit digital word using the ADS1115 analog-to-digital converter. The digital conversion is transferred to the microcontroller using I<sup>2</sup>C data bus.

A propotional-integral-derivative controller (PID controller) was used to control the temperature of LED mounting base. PID controller is a widely used controller in industry due to the simplicity of implementation. It can also be applied on many different tuning problems without knowledge of the details of the process to be controlled [24, p. 1]. PID controller can be implemented using analog electronics or digital microprocessor. In this case, a digital PID controller was used and implemented using ATmega 328 microprosessor with Arduino board.

The PID controller is based on negative feedback loop. In negative feedback, the

manipulated variable moves in an opposite direction to the process variable [24, p. 5]. In this case, the error between the LED forward voltage and the reference voltage is the process variable and pulse width of the power supply driving the thermo electric module (TEM) is the manipulated variable. The set point for the PID controller is zero, thus the controller drives the TEM in such a way that the LED forward voltage equals the reference voltage.

In digital PID controller the measured analog error voltage is digitized and discretized using the analog-to-digital converter. The sampling time for the controller was chosen as 50 ms, thus leaving enough processor resources for signal processing and control algorithm computation.

The PID controller has three gain parameters: propotional gain, integral gain, and derivative gain [24]. Improperly chosen derivative gain can make the controller unstable. Temperature controlling and stabilization do not require fast reaction or transient response, thus the derivative gain was omitted and only proportional and integral terms selected in order to make the controller stable. A PID controller without derivative gain is called PI controller and is typically used for controlling slow processes [24].

The PI controller was implemented on the ATMega 328 microprocessor. In the control algorithm, the processor read the 16-bit digital word from the analog-to-digital converter and filtered the signal using a median filter with a windows size of eleven. The filtered signal was used as an input variable for the controller. The output signal from the controller was a 5 V pulse width modulated signal for a switched mode power supply controlling the thermoelectric module of the LED heat sink (figure 12).



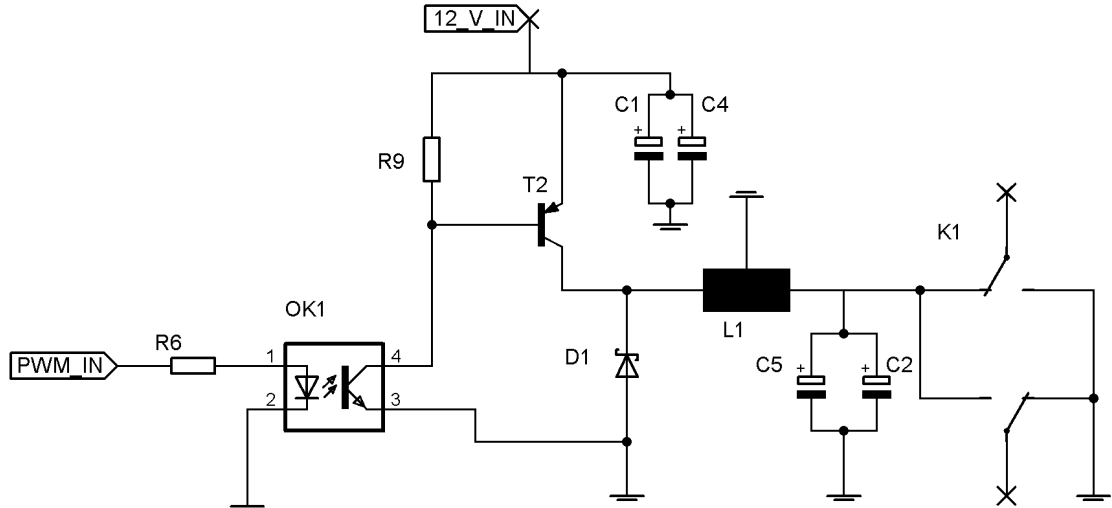


Figure 12: Schematics of the pulse width controlled switched mode power supply for the thermoelectric module of the LED heat sink.

In figure 12, the optically isolated and pulse width modulated control signal from the microprocessor drives the MOSFET transistor "T2". The output voltage of the switched mode power supply is proportional to the pulse width of the control signal. The polarity of the output voltage can be inversed using a relay "K1". Depending on the polarity, the thermoelectric module can either heat or cool the LED mounting. The set point for the LED forward voltage was chosen as 45 V, leading to a LED unit temperature of about 40 °C.

The proportional and integral control parameters for the PI controller were determined using heuristic Ziegler-Nichols tuning method. In the tuning process, the gain parameters were increased until the process started to oscillate and then reduces, until a stable state was achieved.

The control electronics was enclosed into a custom manufactured aluminium enclosure. Figure 13 shows the electronics, connectors, and internal wiring of the control unit.

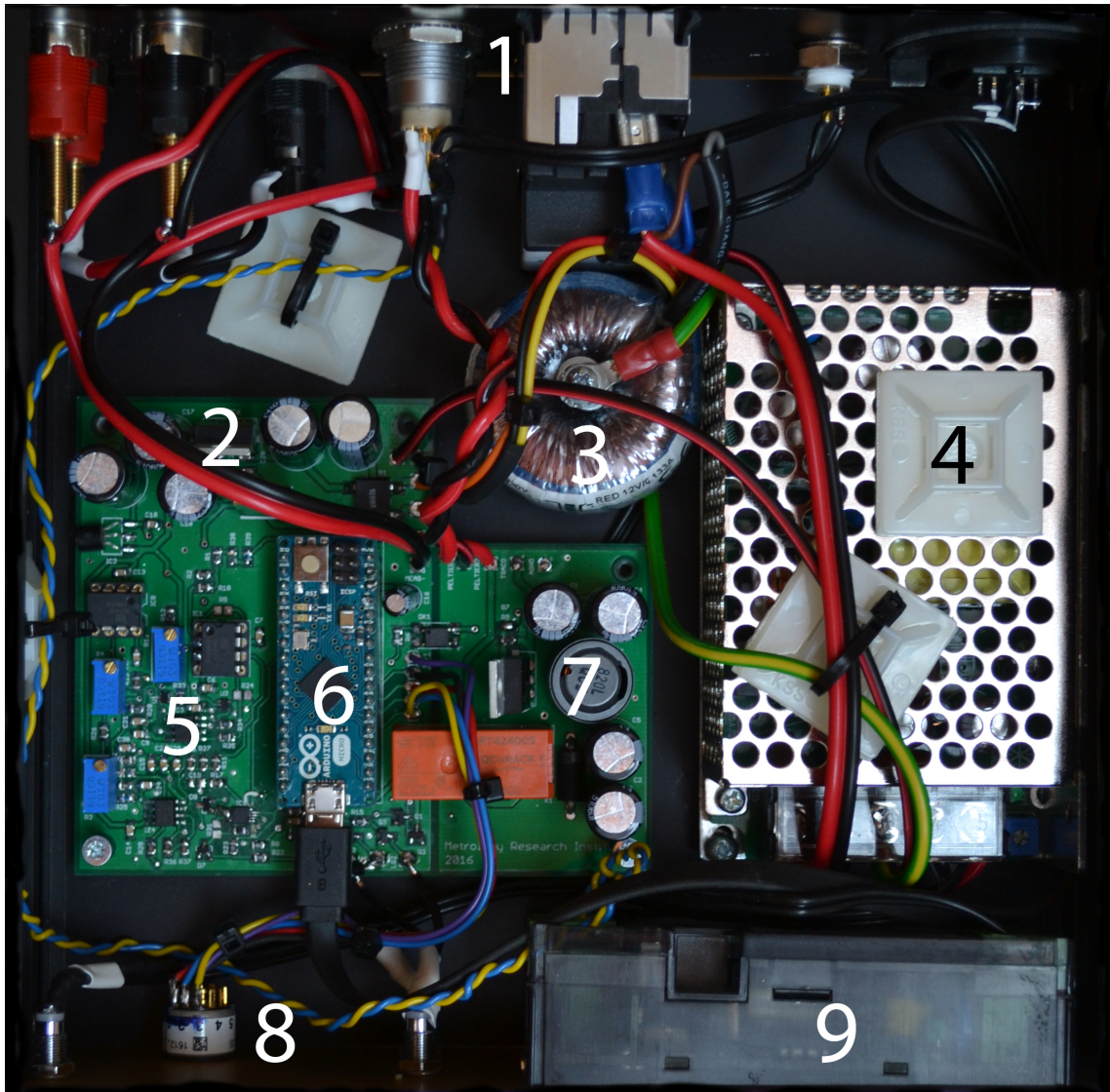


Figure 13: Internal wiring of the control unit.

In the enclosure design, the target was to achieve professional looking, noiseless, and robust device. In the following paragraph the numbers in parenthesis refer to the numbering in figure 13. The wires were arranged in order to prevent inductive disturbances from high current leads inducing to the measurement cables. The sensitive analog electronics (5) was placed as far as possible from the switched mode current source (4) and the switched mode power supply (7) which is also optically isolated from another parts of the circuit. The mains power for the device was supplied through an EMI (electromagnetic interference) filtered power socket (1). The high voltage mains power was reduces using a toroidal transformer (3) preventing electromagnetic interference from disturbing the delicate electronics. The

linear power supply (2) generates the operating voltages for the analog electronics and the microprocessor (6). The front panel (8) of the device comprised of an power LED, two state indicating LEDs, rotary switch to chance the set point, and a stand-alone temperature display (9) showing the temperature of the LED module. The temperature of the LED module is measured using a separate PT-100 temperature sensor which is used only for indicative purposes.

### 3.4 Operating instructions for the LED source

This chapter describes the use for the designed LED-based standard lamp.

1. Mount the standard lamp on the optical rail and align it. The lamp is designed to be compatible with all typical metric mechanic parts.
2. Interconnect the cables between the temperature control unit and the LED unit. Connect the power supply to the control unit. See figure 15 for cable connections
3. Align the lamp to the optical rail using an alignment laser and the optical target of the standard lamp. After alignment, remove the target.
4. Select the desired operating mode by turning the switch on the front panel (see figure 14). Preset 1 is for the cold white LED and preset 2 for the warm white LED. Preset 3 is for the cold white LED with current of 600 mA. This gives 17 % higher intensity compared to using a current of 500 mA, and can be used when higher signal level is required.
5. Turn the constant current LED power supply on. At MRI, the Heinzinger DC power supply is used.
6. Switch on the control unit.
7. Wait for the green "ready" indicator LED to turn on. The "ready" LED should turn on after about 15 minutes from the start.
8. After the "Ready" LED has turned on, the standard lamp is ready for measurements. If "Fault" indicator LED does not turn off during the first 30 minutes from the start the control unit cannot stabilize the LED junction temperature. In such a case, turn off the power and check all cable connections, check that the LED module is tightly screwed on the cooled unit and check the DC power supply settings (Heinzinger). Turn power on and wait to the green led turn on.

Note: Temperature of the LED unit should never rise above 100 ° Celsius. Otherwise, the LED can be damaged. Give attention to the temperature meter and fault-LED and switch the power supply off if temperature rises too high.



Figure 14: The front panel of the Ledstec unit. Power on- LED (1). The preset selector switch (2). The indicator LEDs (3,4) sign to a user if stable condition is achieved or the system has failed. The seven segment screen (5) shows temperature of the heat sink, thus possible changes on LED characteristics can be tracked over the lifetime of the LED standard lamp.

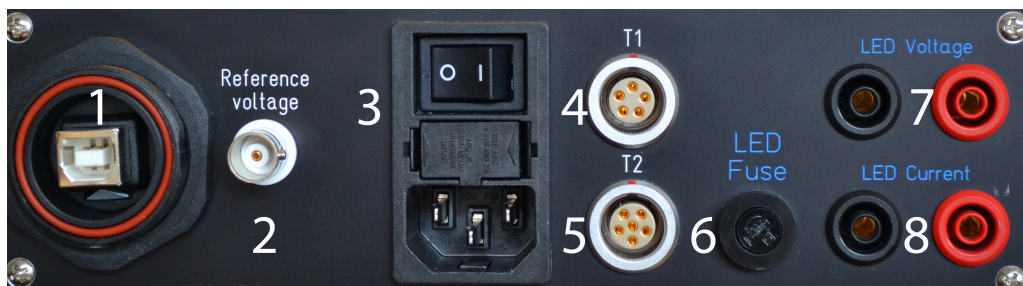


Figure 15: The back panel of the Control unit. Type B USB 2.0 connector (1) for software developing only. "Reference voltage" reference voltage output (2). See chapter 3.4 figure 9. *Schutzkontakt*- style power connector (3) with a fuse and a main switch. "T1" cable terminal (4) for the cooling unit cable. "T2" a cable terminal (5) for the LED unit cable. "LED FUSE" a fuse holder (6) for a 750mA FF fuse which protects the LED from the over current. "LED voltage" LED forward voltage out (7) for an external voltmeter. "LED current" an input connector (8) for an external DC power supply.

## 4 Characterization results

Several test measurements were performed in this work for the new standard lamp: stability of the luminous intensity was tested on the optical rail setup of MRI. The spectral distribution of the LED was measured in the goniospectrometer of MRI and ageing over four months was performed for ten Osram Soleriq LEDs. In addition, the LED standard lamp was used in the characterization as an external source of the integrating sphere of MRI. The methods and results of these measurements are discussed in this chapter.

### 4.1 Ageing test for the LED modules

Stability and ageing of the selected LED modules were tested in order to study the suitability of the module to be used as a luminous intensity standard. Ten Osram Soleriq COB-LEDs were aged in natural conditions for a period of four months. For the purpose, a special automatic ageing setup was built which consisted of a PC computer, a laboratory DC supply and a temperature logging system.

All artefacts were connected in series and driven with 1.0000 A current to ensure that all the artefacts were driven with the same current. The artefacts were operated in such a way, that the LEDs were turned on for 2 hours 45 minutes and then off for 15 minutes in order to cause the thermal stress that emulates switching the lamps off before next set of measurements. The LEDs were mounted on fan cooled heat sinks and the fans were driven by 3.8 V voltage in order to achieve a temperature of 60° Celsius which is about twice of the target temperature of the LED module in normal use of the standard lamp. Figure 16 shows the aged LEDs in their heat sinks.





Figure 16: The ageing test setup. Ten Osram Soleriq LEDs are mounted on heatsinks with active cooling in order to keep the temperature at  $60^{\circ}\text{C}$  during the experiment.

Changes in the artefact properties were measured using the integrating sphere setup of MRI which provides a method for measuring the luminous flux and relative spectral radiant flux of the lamp under test. In this measurement, change in relative luminous flux is equal to the change of intensity.

The measured electrical power [W], luminous flux [lm] and CCT [K] of each artefact in the beginning and in the end of the ageing test are listed in table 3. The luminous flux increased 11 % on the average from round 1 to round 2. Four months equals approximately 2880 hours, which is already more than three times the burn hours of a typical incandescent standard lamp. In addition, the artefacts in the test were operated at the heat sink temperature of  $60^{\circ}\text{C}$  which is twice as much of the temperature of the LED module in real use. That is to say, the changes expected in calibration use are even less than were noticed in this ageing test. At MRI, typical life time of a luminous intensity standard lamp is about 500 hours.

In figures 17 and 18 the spectra of the lamps before and after the ageing period are presented. The luminous flux increased 11 % on the average and CCT decreased 39 K on the average which is 0.8 %.

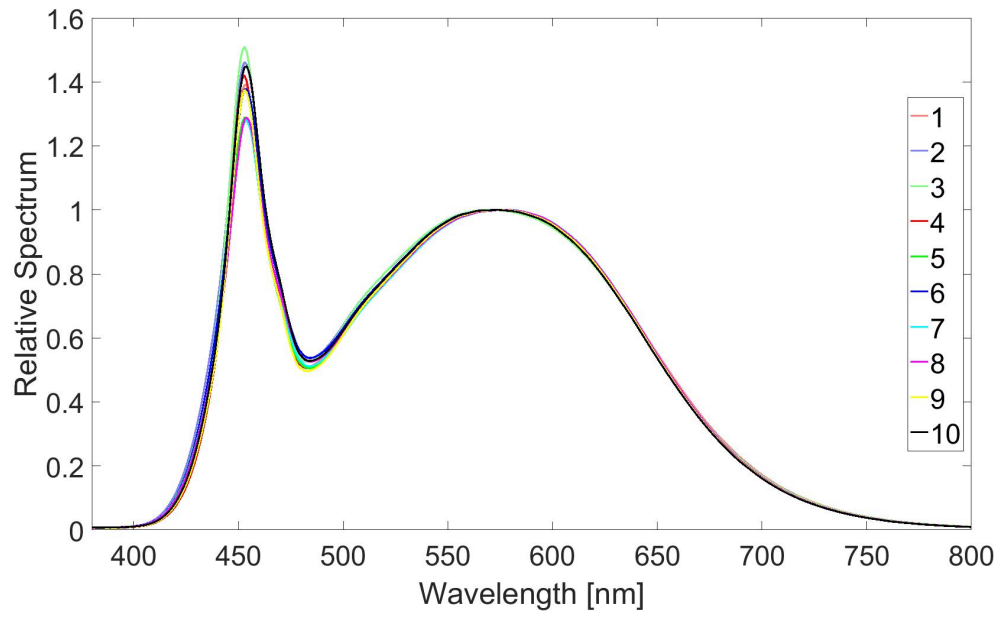


Figure 17: Relative spectra of the cold white Soleriq LED modules before the ageing test.

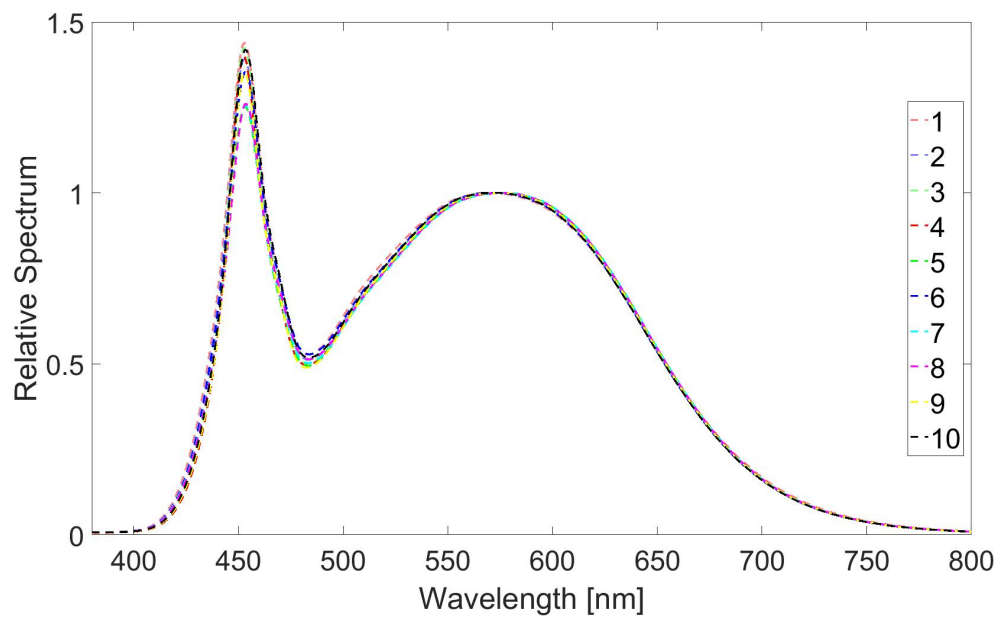


Figure 18: Relative spectra of the cold white Soleriq LED modules after four months of ageing.

Table 3: Results of the ageing study

Lamp	Round 1		Round 2	
	Luminous flux [lm]	CCT [K]	Luminous flux [lm]	CCT [K]
1	3789.81	4904.4	3931.73	5103.3
2	3563.61	5132.5	4043.69	4980.6
3	3783.56	5115.2	3983.91	4945.5
4	3719.85	4858.5	4001.62	4830.7
5	3572.81	4840.6	4083.89	4787.4
6	3636.88	5014.6	4153.96	4976.5
7	3610.32	4797.1	4086.45	4764.2
8	3629.54	4836.0	4114.41	4793.9
9	3471.06	4842.8	3878.19	4813.3
10	3538.61	5021.6	4049.28	4975.2
average	3631.61	4936.3	4032.71	4897.1
stdev %	2.89	2.51	2.10	2.32



## 4.2 Characterization of the LED standard lamp

The developed standard lamp was fully characterised and compared against traditional incandescent standard lamps of type Osram Wi41/G and a FEL-lamp, S.T6. The stability, spectral irradiance, luminous intensity and the applicability of the inverse-square law of all three lamps were measured in order to study if the LED standard lamp was a suitable successor for incandescent standard lamps used in typical photometric calibrations.

The stability was studied by measuring the illuminance of all lamps at the luminous intensity calibration setup of MRI. Figure 19 shows the measured relative illuminance for a period of 75 minutes. Sudden drops on the plots before 500 seconds are caused by fine tuning of the power supply and actual stability measurement starts after that point. The zoomed window shows the short term stability which is stochastic noise for all studied lamps.

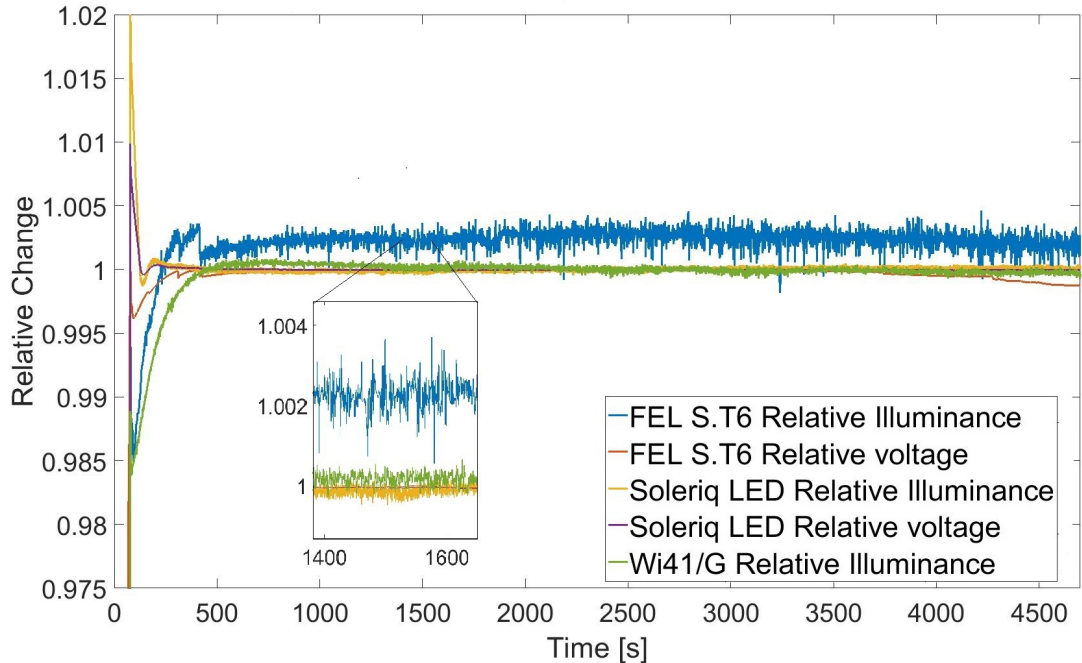


Figure 19: Stability comparison of the developed LED source, FEL S.T6 and Wi41/G luminous intensity standard lamps in a typical calibration situation of 4500 s (75 min) of duration. All lamps were operated in a temperature controlled laboratory room at the ambient temperature of  $23 \pm 0.5$  °C with a pre-warmed Heinzinger DC power supply.

The experiment shows that the LED standard lamp is as good as the WI41/G and about three times more stable than the FEL lamp which is often used in photometry

for higher signal levels, for example, as an external source in the integrating sphere setup of MRI. Spectra of the two Osram Soleriq LEDs, Wi41/G, and the LED illuminants "Lw" and "Lc" published in [1] are presented in figure 20. The correlated colour temperatures were 3158 K for the Osram Soleriq warm white, 5566 K for the Osram Soleriq cold white, 2935 K for the illuminant "L<sub>W</sub>", and 5716 K for the illuminant "L<sub>C</sub>". Despite the spectral shapes are not identical to the analysed illuminants of the study of Pulli et al., the overall spectral shapes of the new standard lamp follow the general characteristics of the two illuminants, thus allowing the greatly reduced spectral errors, as compared to using incandescent lamps in calibration of photometers.

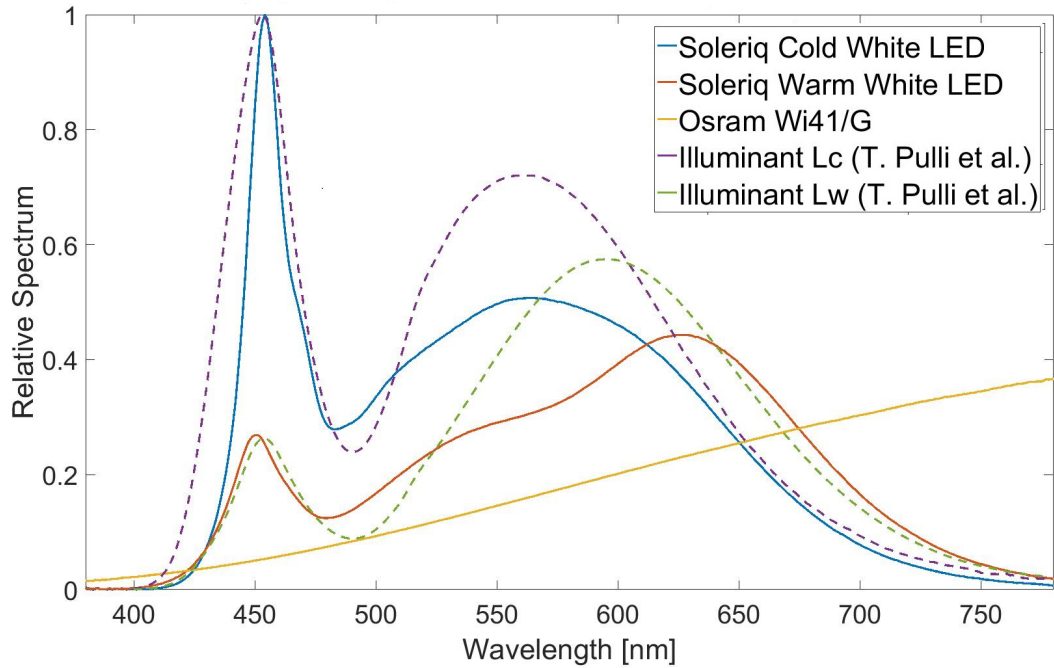


Figure 20: Relative spectra of the two Osram Soleriq LEDs, Wi41/G and the illuminants "L<sub>W</sub>" and "L<sub>C</sub>".

The angular intensity distributions and angular dependency of CCT of the two LEDs with different colour temperatures were measured and compared against Wi41/G. These results of the measurements are shown in figures 21 and 22. The angular distribution of the LEDs are close to the cosine, while the Wi41/G has totally different output due to the limiting output window. Due to the fact that the standard lamp is always measured from the same direction and baffles are typically used, for straylight rejection, the changes in the angular distributions at the high angles of observation are negligible. Nevertheless, a wide main beam or strong side

beams could cause reflections from walls and a ceiling. In MRI, this has been solved by enclosing both the lamp and the detector in a light-tight enclosure that rejects the straylight in the measurement. At the angles from  $-5^\circ$  to  $5^\circ$ , the CCT vary 2 K for the cold white LED, 1 K for the warm white LED and 2 K for the Wi41/G. Thus the variation of the LEDs is similar to the Wi41/G. A more important factor, the colour correction factor  $F$  is three orders of magnitude smaller for the LEDs than for the Wi41/G within angular range of  $-5^\circ$  to  $5^\circ$ : 0.82 % for the Wi41/G, 0.0005 % for the warm white LED and 0.006 % for the cold white LED. According to the angular measurements, alignment rooted uncertainty is as small for the LED than for the incandescent lamp.

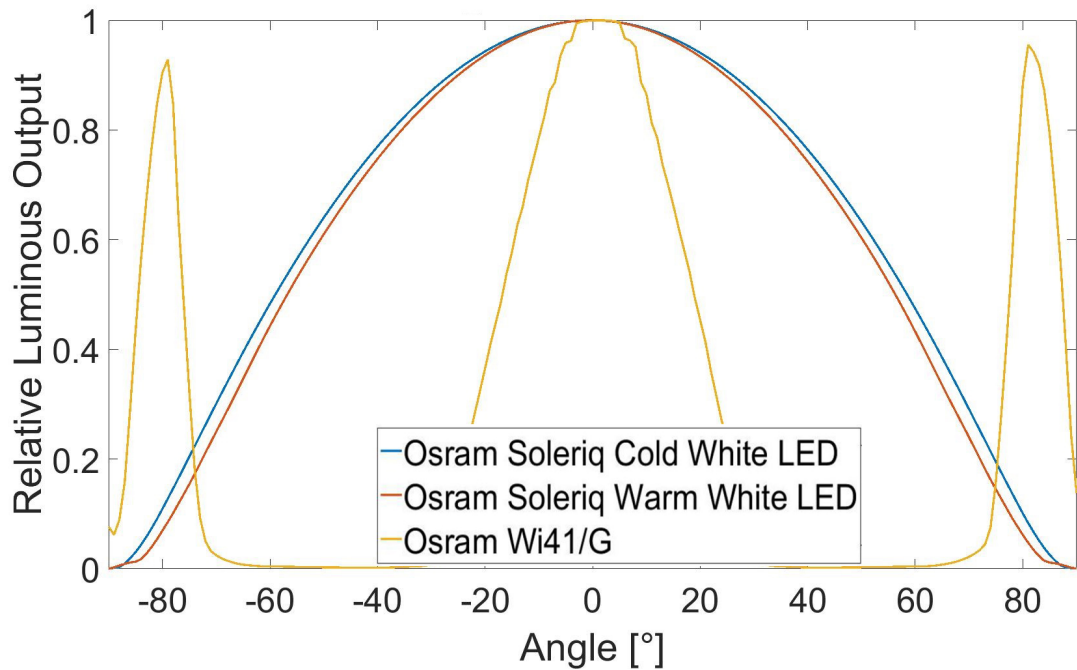


Figure 21: Relative angular intensity distribution of the LED standard lamp and the Wi41/G. Both Osram Soleriqs have a cosine-type of distribution. The Wi41/G has strong main and side lobes because of black paint of its glass envelope.

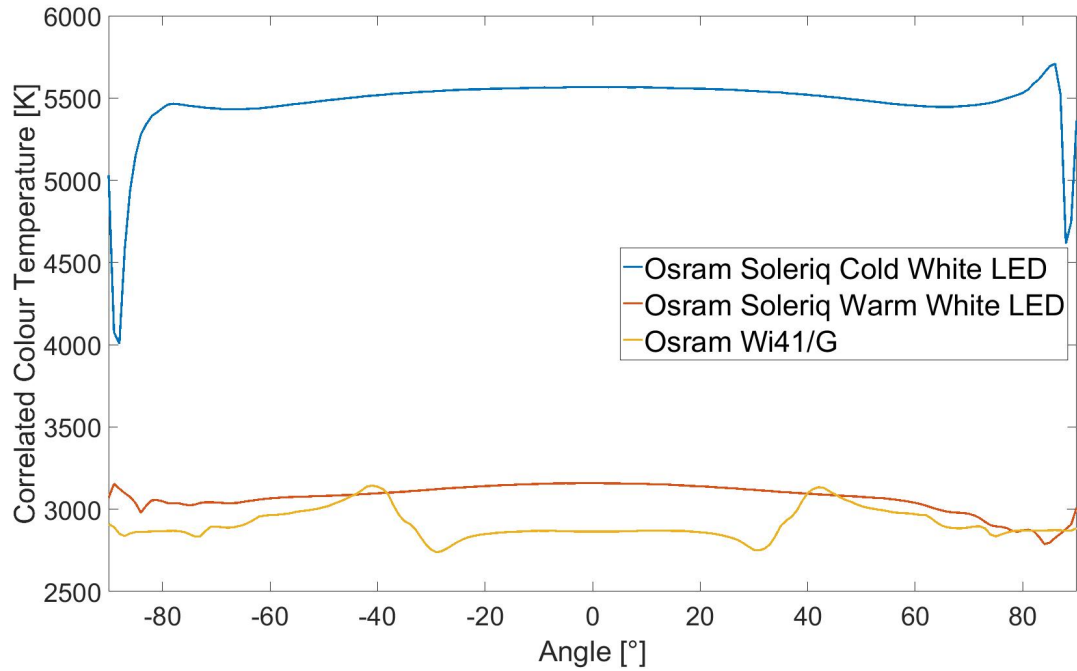


Figure 22: Colour temperatures of the two Osram Soleriq LEDs and the Wi41/G incandescent standard lamp measured in angular range from  $-90^\circ$  to  $90^\circ$  with  $1^\circ$  steps. The changes of colour temperatures for all three lamps are almost the same within the range from  $-20^\circ$  to  $20^\circ$ .

### 4.3 Measurement of luminous intensity

The luminous intensity of the developed standard lamp was measured using the luminous intensity setup of MRI. In these measurements, the illuminance of the LED source was measured at five different distances from the source within a range of 0.5 - 4.0 m. The measurement setup for luminous intensity has been described in more details in Chapter 2.2. The luminous intensity was measured according to the agreed methods of the laboratory. The expanded uncertainty of the luminous intensity measurement of the LED standard lamp is 0.62 % ( $k = 2$ ). The uncertainty budget is presented in the table below.

### Uncertainty budget for luminous intensity measurement

Source of uncertainty	%
Photometer responsivity	0.19
Colour correction factor $F$	0.002
Aperture area	0.17
Stability of the source	0.10
Alignment of the source	0.01
Distance measurement	0.05
Repeatability	0.14
Combined standard uncertainty	0.31
Expanded uncertainty ( $k = 2$ )	0.62

The component due to the photometer responsivity includes uncertainties arising from the absolute spectral responsivity, non-linearity and spatial non-uniformity of the photo-detector, and of the transmittance of the  $V(\lambda)$ -filter. These components of the photometer have been individually characterised using the methods described in [25].

The colour correction factor  $F$ , stability of source and repeatability were studied by measurements. The uncertainty due to  $F$  was calculated by inspecting the differences in the measured spectra of the source between  $-0.2^\circ$  and  $0.2^\circ$  angles of observation, and a simulated effect of 1 nm wavelength shift in the spectral measurement, and the resulting differences in the obtained correction factors  $F$ . The effect of angular alignment error was only 0.00023 % in  $F$ , while the shift of 1 nm in wavelength causes a difference of 0.0015 % in  $F$ . The wavelength shift of 1 nm is slightly conservative, but it is expected to include also other sources of error in spectral measurement. The final uncertainty due to  $F$  was calculated as a sum of squares of these two values.

The uncertainty due to the aperture diameter ( $2.9971 \pm 0.005$  mm) is based on the uncertainty stated in the calibration certificate M-16L055 of MIKES [26].

The short term temporal stability of the source was studied by measuring the LED on the optical rail setup of MRI with the reference photometer for a time period of 1.5 hours. The uncertainty due to the stability of the source was calculated as a relative standard deviation of the measured illuminance values between 15 - 75 min from the beginning of the measurement.

The uncertainty due to the alignment of the source, and the resulting difference in measured illuminance, was obtained by measuring the angular intensity distribution of the LED source with the goniospectrometer.

Uncertainty due to the distance measurement is based on the resolution (0.1 mm) and calibration certificate M-08L356 [27] of the magnetic distance measurement rail of MRI.

The measurement was repeated five times on different days in order to determine the repeatability of the measurement, and to evaluate the uncertainty budget for the luminous intensity. Between the measurements, the light source and the photometer were disassembled, reassembled and aligned again.

#### 4.4 Calibration of the integrating sphere

Luminous flux is an important quantity in the field of photometry. Integrating sphere is one method to measure and realize the luminous flux in the industry and in national metrology institutes. For example, at MRI the integrating sphere is used commonly in every day study for measurements of solid state lighting products, such as LED bulbs, OLED panels, street lights and other typical light sources.

The luminous flux measurement setup is presented in figure 23. The setup consists of an integrating sphere, a photometer and auxiliary characterization devices. The integrating sphere consists of two aluminium hemispheres which are painted with barium sulfate ( $\text{BaSO}_4$ ) paint inside in order to achieve a highly reflecting surface with Lambertian reflection. The sphere has a detector port for the measurement device, such as a photometer or a spectrometer and one or more auxiliary ports for characterization and calibration of the setup. The test lamp is placed in the holder in the centre of the sphere. Input luminous flux to the sphere is measured with the reference photometer and output from the sphere is measured with another photometer from the main port of the sphere.

Luminous flux and relative spectral radiant flux are measured using a photometer with a current-to-voltage converter, a digital voltmeter and a spectrometer. In the measurements, the luminous flux of the test lamp is compared against the luminous flux produced by the external source [6, 28, 29].

The LED based standard lamp can be used in calibration of the luminous flux responsivity of the integrating sphere as a stable external source. Previously, this has been done using a 1 kW FEL lamp. The luminous flux responsivity of the sphere was calibrated at first with the FEL and then with the LED standard lamp in order to examine the possible differences caused by a different type of external source. The main interests were the differences in obtainable signal levels measured with the sphere photometer.

The illuminance of the external source is measured with a standard photometer which is placed in front of the reference entrance of the sphere. The area of the

beam is limited using a precision aperture array between the external source and the entrance of the integrating sphere. The signal level of the sphere photometer is measured with a working standard photometer, which has a cosine-corrected entrance diffuser. The purpose of the baffles is to prevent the detector port from directly seeing the light source under measurement (baffle 2), and preventing the light from escaping through the reference entrance port (baffle 1).

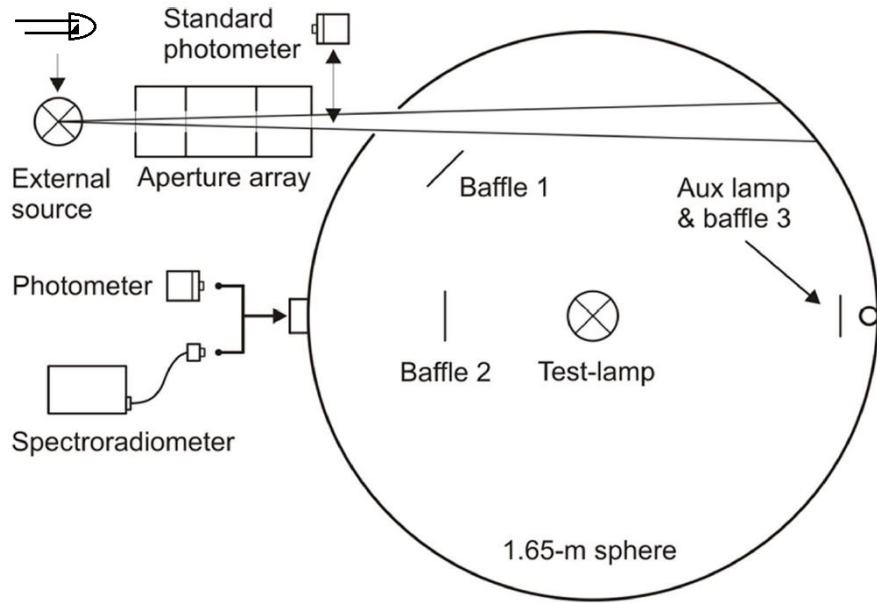


Figure 23: Integrating sphere for luminous flux measurement of SSL products. In addition to the photometer, a spectroradiometer can be connected to the main port for spectral measurements. The aux lamp can be used for the self-absorption measurement of the test lamp. [30]

The luminous flux responsivities obtained for the sphere were 7.939 nA/lm and 7.660 nA/lm with the FEL and LED source, respectively. The difference of about 3.6 % of the measured responsivities originates from the spectral properties of the two sources. In the measurements, the sphere photometer signal with the LED source was 3.9 % higher compared to using the FEL as an external source. Based on these results, the new LED source is equal or better than the FEL when considering the signal-to-noise ratio of the measurement. In these measurements the external LED source was driven with 600 mA current. The situation is even better for the LED when operated with the higher current, up to 1.000 A for the Osram Soleriq.

Calibrating the integrating sphere with the LED standard lamp allows measurement of SSL products with similar CCT and reduced colour correction factors. In



addition, the spectral effects, such as fluorescence due to the blue LEDs used in SSL product are perceived more equally with the LED standard lamp, as compared to using the FEL in the calibrations.

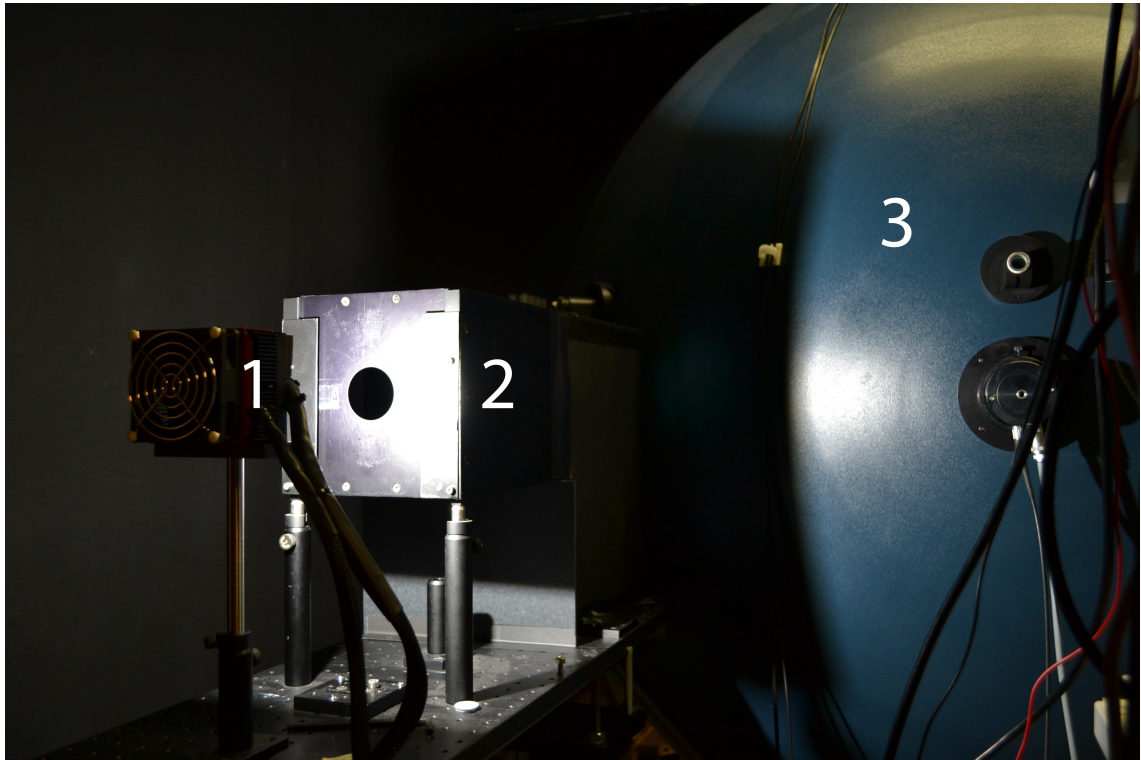


Figure 24: The LED standard lamp (1) as an external calibration source of the integrating sphere (3). The light is limited using an aperture series (2) before entering the sphere.



## 5 Conclusions

In this work, an LED-based luminous intensity standard lamp was designed, built, and characterized for calibrations of photometric equipment. The goal of the work was to design a mechanically backwards compatible LED standard lamp to replace obsolete incandescent standard lamps used in photometry. The optical properties of the developed LED standard lamp were chosen to be comparable with the incandescent standard lamps, except spectral properties that allow reduced uncertainties in measurements of SSL products with similar colour temperature. The mechanics of the lamp allow it to be used in measurements in the same way as all typical standard lamps used in photometry.

The stability and stabilization time of the LED standard lamp were measured and compared against Osram Wi41/G and FEL S.T6 lamps. According to the comparison, the LED standard lamp performs at least as well as the Wi41/G and better than the FEL. The standard deviations calculated from the illuminance measurements of the source between 10 - 75 minutes from the beginning of the measurement were 1.14 times higher for the Wi41/G, three times higher for the FEL, as compared to the LED standard lamp. The test calibration of the integrating sphere showed that the LED-based lamp works as well as the FEL as an external source and allows even higher signal levels depending on the operating current. Ageing test with a duration of 2880 hours showed no significant drop in the average luminous flux of the Osram Soleriq LED modules tested at 60 °C. This duration already corresponds to at least five times of the typical life time of an incandescent standard lamp.

The expanded uncertainty of the luminous intensity measurement of the LED standard lamp is 0.62 % ( $k = 2$ ). The standard lamp will be utilized as a calibration source in future research projects addressing the issues of classical photometry, and development of new measurement methods for measurement and testing of SSL-products coming to market.

## References

- [1] T. Pulli, T. Dönsberg, T. Poikonen, F. Manoocheri, P. Kärhä, and E. Ikonen, “Advantages of white led lamps and new detector technology in photometry,” *Light: Science & Applications*, vol. 4, no. 9, p. e332, 2015.
- [2] J.-M. Hirvonen, T. Poikonen, A. Vaskuri, P. Kärhä, and E. Ikonen, “Spectrally adjustable quasi-monochromatic radiance source based on leds and its application for measuring spectral responsivity of a luminance meter,” *Measurement Science and Technology*, vol. 24, no. 11, p. 115201, 2013.
- [3] F. Sametoglu, “Influence of the spectral power distribution of a led on the illuminance responsivity of a photometer,” *Optics and Lasers in Engineering*, vol. 46, no. 9, pp. 643–647, 2008.
- [4] I. Fryc, S. Brown, and Y. Ohno, “Spectral matching with an led-based spectrally tunable light source,” in *Optics & Photonics 2005*, pp. 59411I–59411I, International Society for Optics and Photonics, 2005.
- [5] P. Giacomo, “News from the bipm,” *Metrologia*, vol. 16, no. 1, p. 55, 1980.
- [6] T. Poikonen, T. Pulli, A. Vaskuri, H. Baumgartner, P. Kärhä, and E. Ikonen, “Luminous efficacy measurement of solid-state lamps,” *Metrologia*, vol. 49, no. 2, p. S135, 2012.
- [7] J. Hovila, Jovila, P. Manninen, T. Poikonen, and T. Pulli, “Quality manual of luminous intensity laboratory,” 2015.
- [8] A. Sperling, G. Sauter, D. Lindner, and M. Eltmann, “Euramet key-comparison luminous intensity euramet.pr.k3.a final report, may 2014,” tech. rep., Physikalisch-Technische Bundesanstalt, Germany, 2014.
- [9] C. Cromer, G. Eppeldauer, J. E. Hardis, T. C. Larason, Y. Ohno, and A. C. Parr, “The nist detector-based luminous intensity scale,” *JOURNAL OF RESEARCH-NATIONAL INSTITUTE OF STANDARDS AND TECHNOLOGY*, vol. 101, pp. 109–132, 1996.
- [10] G. Sauter, “Review on new developments in photometry,” *Proc. NEWRAD, Davos, Switzerland*, 2005.
- [11] Y. Ohno, “Detector-based luminous-flux calibration using the absolute integrating-sphere method,” *Metrologia*, vol. 35, no. 4, p. 473, 1998.

- [12] G. Sauter, “Goniophotometry: new calibration method and instrument design,” *Metrologia*, vol. 32, no. 6, p. 685, 1995.
- [13] IESNA, *Lighting Handbook*. IESNA, 1993.
- [14] E. F. Schubert, ed., *Light-Emitting Diodes*. New York: Cambridge University Press, 2003.
- [15] “Measurement of leds,” tech. rep., International Commission on Illumination, 1997.
- [16] P. Manninen, J. Hovila, P. Kärhä, and E. Ikonen, “Method for analysing luminous intensity of light-emitting diodes,” *Measurement Science and Technology*, vol. 18, no. 1, p. 223, 2006.
- [17] S. Ishizaki, H. Kimura, and M. Sugimoto, “Lifetime estimation of high power white leds,” *Journal of Light & Visual Environment*, vol. 31, no. 1, pp. 11–18, 2007.
- [18] H. Baumgartner, D. Renoux, P. Kärhä, T. Poikonen, T. Pulli, and E. Ikonen, “Natural and accelerated ageing of led lamps,” *Lighting Research and Technology*, p. 1477153515603757, 2015.
- [19] N. Narendran, Y. Gu, J. Freyssinier, H. Yu, and L. Deng, “Solid-state lighting: failure analysis of white leds,” *Journal of Crystal Growth*, vol. 268, no. 3, pp. 449–456, 2004.
- [20] S. Hui and Y. Qin, “A general photo-electro-thermal theory for light emitting diode (led) systems,” *Power Electronics, IEEE Transactions on*, vol. 24, no. 8, pp. 1967–1976, 2009.
- [21] F.-K. Wang and T.-P. Chu, “Lifetime predictions of led-based light bars by accelerated degradation test,” *Microelectronics Reliability*, vol. 52, no. 7, pp. 1332–1336, 2012.
- [22] F. Steranka, J. Bhat, D. Collins, L. Cook, M. Craford, R. Fletcher, N. Gardner, P. Grillo, W. Goetz, M. Keuper, *et al.*, “High power leds—technology status and market applications,” *physica status solidi (a)*, vol. 194, no. 2, pp. 380–388, 2002.
- [23] “Ads1115 ultra-small, low-power, 16-bit analog-to-digital converter with internal reference,” tech. rep., Texas Instruments Incorporated, 2013.

- [24] K. Aström and T. Hägglund, *Advanced PID Control*. ISA - The Instrumentation, Systems and Automation Society, 2006.
- [25] P. Toivanen, J. Hovila, P. Kärhä, and E. Ikonen, “Realizations of the units of luminance and spectral radiance at the hut,” *Metrologia*, vol. 37, no. 5, p. 527, 2000.
- [26] MIKES, “Certificate of calibration m-16l055,” 2016.
- [27] MIKES, “Certificate of calibration m-08l356,” 2008.
- [28] Y. Ohno, “New method for realizing a luminous flux scale using an integrating sphere with an external source,” *Journal of the Illuminating Engineering Society*, vol. 24, no. 1, pp. 106–115, 1995.
- [29] J. Hovila, P. Toivanen, and E. Ikonen, “Realization of the unit of luminous flux at the hut using the absolute integrating-sphere method,” *Metrologia*, vol. 41, no. 6, p. 407, 2004.
- [30] T. P. J. Hovila, P. Manninen, “Quality manual of luminous flux measurements,” *Aalto University, School of Electrical Engineering*, 2014.